Molecular Ecology (2009) **18**, 2574–2587 doi: 10.1111/j.1365-294X.2009.04220.x

Gene flow by larval dispersal in the Antarctic notothenioid fish *Gobionotothen gibberifrons*

MICHAEL MATSCHINER,* REINHOLD HANEL† and WALTER SALZBURGER*
*Zoological Institute, University of Basel, Vesalgasse 1, CH-4051 Basel, Switzerland, †Institute of Fisheries Ecology, Johann Heinrich von Thünen-Institut, Federal Research Institute for Rural Areas, Forestry and Fisheries, Palmaille 9, D-22767 Hamburg, Germany

Abstract

The diversification of the teleost suborder Notothenioidei (Perciformes) in Antarctic waters provides one of the most striking examples of a marine adaptive radiation. Along with a number of adaptations to the cold environment, such as the evolution of antifreeze glycoproteins, notothenioids diversified into eight families and at least 130 species. Here, we investigate the genetic population structure of the humped rockcod (*Gobionotothen gibberifrons*), a benthic notothenioid fish. Six populations were sampled at different locations around the Scotia Sea, comprising a large part of the species' distribution range ($N = 165$). Our analyses based on mitochondrial DNA sequence data (352 bp) and eight microsatellite markers reveal a lack of genetic structuring over large geographic distances ($\Phi_{ST} \leq 0.058$, $F_{ST} \leq 0.005$, P values nonsignificant). In order to test whether this was due to passive larval dispersal, we used GPS-tracked drifter trajectories, which approximate movement of passive surface particles with ocean currents. The drifter data indicate that the Antarctic Circumpolar Current (ACC) connects the sampling locations in one direction only (west–east), and that passive transport is possible within the 4-month larval period of *G. gibberifrons*. Indeed, when applying the isolation-with-migration model in IMA, strong unidirectional west-east migration rates are detected in the humped rockcod. This leads us to conclude that, in *G. gibberifrons*, genetic differentiation is prevented by gene flow via larval dispersal with the ACC.

Keywords: adaptive radiation, population genetics, isolation-with-migration model, drifters

Received 15 December 2008; revised 25 March 2009; accepted 27 March 2009

Introduction

Adaptive radiation is the evolution of ecological and morphological diversity within a rapidly multiplying lineage (Schluter 2000). Only very few adaptive radiations are known from the marine realm, which is surprising given the numerous examples of adaptive radiations in freshwater systems (Salzburger 2009). One explanation for this observation could be that adaptive radiations are simply more apparent in geographically well-defined areas such as islands or lakes and less detectable in open systems such as oceans (Salzburger 2008). Some adaptive radiations in marine fishes are indeed characterized by their geographic circumscription. The colourful hamlet species complex (*Hypoplectrus*; family Serranidae), for example, is confined to the Caribbean Sea, where about a dozen of species have rather recently emerged (Puebla *et al*. 2008). Among the most species-rich marine adaptive radiations in teleosts is the one of notothenioid fishes in Antarctic waters that diversified into at least 130 species (Eastman 2005; Cziko & Cheng 2006). Today, the notothenioids dominate the Antarctic continental shelf and upper slope in terms of species number (47%) and fish biomass (90–95%) (Eastman & Clarke 1998). Antarctic shelf areas are separated from other continental shelves by the Antarctic Circumpolar Current (ACC) that reaches the ocean floor (Foster 1984) and transports more water than any other ocean current (Tomczak & Godfrey 2003). The Antarctic Polar Front (APF), among other oceanic frontal zones, delimits the Southern Ocean (Kock 1992), posing an oceanographic barrier to marine organisms and thermally isolating the continent (Shaw *et al*. 2004).

The remarkable diversification of the Notothenioidei has been accompanied by several morphological adaptations

Correspondence: W. Salzburger, Fax: +41 61 267 03 01, E-mail: walter.salzburger@unibas.ch

and evolutionary innovations. Presumably most important for the adaptation to the Antarctic environment was the evolution of antifreeze glycoproteins from a trypsinogen progenitor (Chen *et al*. 1997). In the freezing waters of Antarctica, these proteins bind to the surface of forming ice crystals in blood and tissue and thus inhibit their further growth (DeVries 1988). On the other hand, some notothenioids lack otherwise common features. For example, the channichthyid family is characterized by the inability to synthesize haemoglobin, which is unique among vertebrates (Kock 2005). Channichthyidae have adapted to the lack of respiratory pigments with increased blood volume and cardiac output while at the same time maintaining a low metabolic rate. In addition, the mitochondrial ND6 gene (coding for NADH subunit 6) went amiss in notothenioids of the 'Antarctic clade' (Papetti *et al*. 2007a), and swim bladders are absent in all notothenioids (Eastman 1993). Reasons for the persistence of these presumably deleterious traits are difficult to interpret, and their influence on the notothenioid radiation is not yet known (Sidell & O'Brien 2006; Papetti *et al*. 2007a).

Here, we investigate the population structure of the humped rockcod (*Gobionotothen gibberifrons*), a benthic notothenid with a depth range down to 750 m (Eastman 2005; Kompowski 1985). It is distributed along the northwestern Antarctic Peninsula (AP), around the South Shetland Islands including Elephant Island, the South Orkney Islands, and the islands and sea mounts of the Scotia Ridge (SR), including South Georgia (Fig. 1; DeWitt *et al*. 1990). The species spawns small eggs of around 2 mm in diameter in July and August during the austral winter. After 2 to 3 months of incubation, hatching occurs in October when larvae are *c*. 8 mm in length. Larvae become pelagic and feed mainly on copepods in the upper 100 m of the water column. The end of the larval phase is reached by mid-January to early February, at a standard length of 25 mm when most fin-rays are developed. The early juvenile stages return to a demersal lifestyle before the first winter (North 2001).

Characteristics of *G. gibberifrons* habitats differ between the AP and the SR. Due to its lower latitude, South Georgia water temperatures are higher than those at the AP over at least a part of the *G. gibberifrons* depth range. Furthermore, temperature variability decreases with latitude (Barnes *et al*. 2006). As a result of the later onset of the production cycle, *G. gibberifrons* spawning and hatching times at AP locations are delayed by about 1 month compared to South Georgia (Kock & Kellermann 1991). In addition, nutrient content of seawater differs between the two locations, with higher levels of nitrate and silicic acid being available at the AP (Silva S. *et al*. 1995; Whitehouse *et al*. 1996). It could thus be expected that local adaptation led to genetic differentiation between AP and SR populations. To test this hypothesis, we analysed the population genetic structure of six *G. gibberifrons* populations around the Scotia Sea using mitochondrial and nuclear DNA markers. Combining molecular and oceanographic data, we then evaluate whether adult migration or larval dispersal are agents of gene flow in Antarctic waters. We were particularly interested in the question whether neutral drift and/or gene flow affect local adaptation in notothenioids. This was based on the observation that in many adaptive radiations, the interplay of barriers

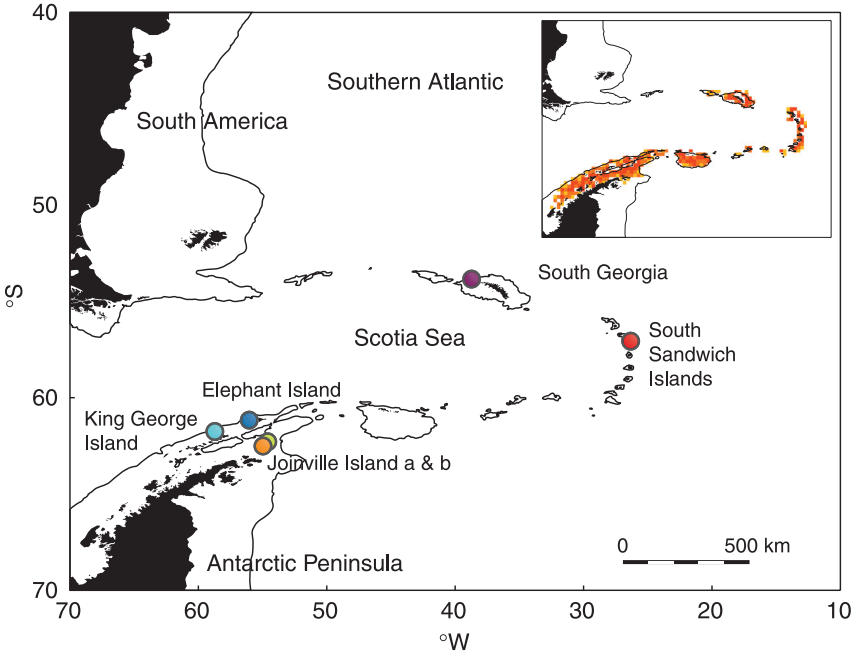

Fig. 1 *Gobionotothen gibberifrons* sampling sites at the tip of the AP, South Georgia, and the South Sandwich Islands. The solid line indicates the 1000-m depth contour. Inset: *G. gibberifrons* distribution range.

Table 1 Sampling sites for *Gobionotothen gibberifrons* around the Scotia Sea. Mean values are given for latitude, longitude and depth. *n*, sample size

Location	Latitude	Longitude	Depth	*n*
Elephant Island	61°13′S	55°53′W	144 m	49
Joinville Island A	62°15′S	55°18′W	356 m	30
Joinville Island B	62°26′S	55°37′W	240 m	33
King George Island	61°51′S	59°14′W	267 m	35
South Georgia	53°48′S	38°43′W	255 m	8
South Sandwich Islands	57°04′S	26°47′W	118 m	10

to gene flow and local adaptation are driving forces for allopatric (or parapatric) speciation (see, e.g. Mayr 1984; Schluter 2000; Rico & Turner 2002).

Materials and methods

Sample collection and DNA extraction

Sampling of *Gobionotothen gibberifrons* specimen was undertaken as part of the ICEFISH 2004 cruise with RV Nathaniel B. Palmer (Jones *et al*. 2008), and during expedition ANT-XXIII/8 with RV Polarstern in the austral summer 2006/2007. In total, 165 specimens were available from six locations around the Scotia Sea (Fig. 1 and Table 1). Muscle or fin tissue samples were taken from all specimens and preserved in 95% ethanol. Genomic DNA was extracted from *c*. 25 mm^3 of muscle or fin tissue using the BioSprint 96 workstation (QIAGEN) according to the manufacturer's guidelines.

Mitochondrial DNA: D-loop

The hypervariable 3′ end of the mitochondrial control region was amplified in polymerase chain reactions (PCRs) using primers LPR-02 and HDL2 (Derome *et al*. 2002). The PCR mixture contained 2 μL template DNA, 3.5 mM $MgCl_2$, 1.0 mM of each nucleotide, 0.2 μM of each primer, 2.5 U *Taq* polymerase (QIAGEN) in 25 μL 1× PCR buffer (QIAGEN) containing Tris-Cl, KCl and $(NH_4)_2SO_4$ and adjusted to pH 8.7 (20°C). Amplifications were performed in a Veriti thermal cycler (Applied Biosystems) with a cold-start PCR profile consisting of an initial predenaturation phase (3 min, 94°C), followed by 35 cycles of denaturing (30 s, 94°C), annealing (30 s, 52°C) and elongation phase (90 s, 72°C), and a final extended elongation phase (7 min, 72°C). PCR purification was done using the GenElute PCR Clean-Up kit (Sigma-Aldrich), following the manufacturer's protocol. Cycle sequencing was performed in forward direction using the BigDye Terminator version 3.1 Cycle Sequencing kit (Applied Biosystems), according to the manufacturer's instructions. Sequencing products were purified by sodium acetate precipitation and run on a 3130 Genetic Analyzer (Applied Biosystems).

Sequence analysis resulted in an alignment of 162 sequences. The alignment was collapsed, but information about the frequency of haplotypes was kept. MODELTEST 3.7 (Posada & Crandall 1998) was run on the collapsed alignment to determine the best-fitting model of sequence evolution. Phylogenetic tree reconstruction was done using the maximum-likelihood method implemented in PAUP* 4.0b10 (Swofford 2003), and the model of sequence evolution selected by likelihood ratio test, HKY + Γ (Hasegawa *et al*. 1985). On the basis of the inferred phylogenetic tree, a haplotype genealogy was constructed.

A distance matrix of all haplotypes was calculated from this genealogy, and used in a hierarchical analysis of molecular variance (AMOVA) in order to compare genetic variation within populations, within predefined groups and among groups. Two different weighting schemes of transitions and transversions were applied: (i) using even weights, and (ii) taking into account the observed ratio of 2:1. In both cases, all possible groupings were assessed and ranked by among group variation. In addition, analogues to Wright's (1978) *F*-statistics were calculated in pairwise comparisons of all populations. Both analyses were done with ARLEQUIN 3.11 (Excoffier *et al*. 2005) and running 10 000 permutations.

The statistical power of the mitochondrial DNA (mtDNA) data set was assessed using POWSIM 4.0 (Ryman & Palm 2006). This software estimates the probability of false negatives for population differentiation, given an expected degree of divergence. Simulations were run with various combinations of N_e (effective population size) and t (time since divergence) to yield F_{ST} values of 0.001, 0.0025, 0.005, 0.01, and 0.02, both on a global level including all populations, and between pooled AP and SR populations. For every simulation, 1000 replicates were run, and default parameters were used for the number of dememorizations, batches, and iterations per batch.

The demographic history of *G. gibberifrons* was tested at the species level, with a mismatch analysis (Li 1977) of all 162 D-loop sequences. The distribution of pairwise mutational distances was fitted to a model of instantaneous population expansion by a generalized nonlinear least-square procedure as implemented in ARLEQUIN, taking into account the observed transition to transversion ratio. The validity of this model was tested by a parametric bootstrap approach running 10 000 bootstrap replicates. Time of population expansion (scaled by mutation rate) was estimated directly from the mismatch distribution and translated into absolute time in years (t_e), using the equation $t_e = \tau/2\mu$, where μ is the mutation rate per locus per year. We used a mutation rate of 6.5–8.8% per million years (Myr) that was found in perciform fishes for the 3′ end of the mitochondrial control region (Sturmbauer *et al*. 2001).

Similar rates have been found in damselfishes (6.9–7.8%; Domingues *et al*. 2005), sculpins (9%; Volckaert *et al*. 2002), and salmonids (5–10%; Brunner *et al*. 2001).

Nuclear DNA: microsatellites

Nine microsatellite loci were cross-amplified using primers isolated from other notothenioid species (Table S1, Supporting information). Loci Trne35, Trne37, Trne53 and Trne66 were isolated from a nototheniid relative, *Trematomus newnesi* (van Houdt *et al*. 2006), while Cr38, Cr127, Cr170, Cr259 and Ca26 have been isolated from channichthyid notothenioids, *Chionodraco rastrospinosus* and *Chaenocephalus aceratus* (Papetti *et al*. 2006; Susana *et al*. 2007). With the exception of Cr127 and Cr259 (Papetti *et al*. 2007b), none of the loci have been cross-amplified before. All forward primers were fluorescently labelled. Amplifications were done in total volumes of 10 μL using the QIAGEN Multiplex PCR kit.

Individual amplification volumes contained 0.8 μL template DNA, 0.2 μM forward and reverse primers in 1× QIAGEN Multiplex PCR Master Mix comprising HotStar *Taq* DNA Polymerase, nucleotides and 3 mM $MgCl_2$. DNA polymerase was activated in an initial activation step (15 min, 95°C), followed by 31–37 thermocycles (see Table S1) of denaturation (30 s, 94°C), annealing (90 s, 59° or 60°C) and extension phase (90 s, 72°C), and a final extension (10 min, 72°C). Amplified products were processed on a 3130 Genetic Analyzer (Applied Biosystems) with LIZ500 size standard (Applied Biosystems).

Microsatellite data were further analysed using GENEMAPPER, version 4.0 (Applied Biosystems). All fragment sizes were automatically pre-analysed by the software and checked by eye. Data of 164 individuals met the quality criteria. We used TANDEM, version 0.9 (Matschiner & Salzburger 2009) for automated binning of allele sizes.

Binned alleles were statistically analysed using ARLEQUIN. Locus Cr170 was found to be monomorphic and was excluded from all further analyses. Pairwise tests of linkage disequilibrium (Slatkin 1994; Slatkin & Excoffier 1996) were performed on the eight remaining loci, running 1000 permutations. The software MICROCHECKER (Van Oosterhout *et al*. 2004) was used to test for null alleles, stuttering and large allele dropout. In addition, an analysis of molecular variance (AMOVA) was conducted, and *F*-statistics were calculated, again as implemented in ARLEQUIN. Ten thousand permutations were performed in both cases. Again, all possible groupings of the hierarchical AMOVA were assessed.

A population assignment test was carried out using the Bayesian model-based clustering method implemented in the software STRUCTURE (Falush *et al*. 2007). The admixture model with standard settings was applied and 100 000 Markov chain Monte Carlo steps, with a burn-in period of 10 000, were used. Six runs were done to test for the number of genetic clusters, *K*, in the data set ($1 \leq K \leq 6$). Every run was repeated three times to assess convergence. Resulting log-likelihoods were compared between values of *K* to determine the actual number of population partitions.

Statistical power analyses were conducted with POWSIM 4.0, using the same settings as for the mtDNA data set.

Drifter analysis

In order to investigate possible means of gene flow in the Scotia Sea, the trajectories of satellite-tracked drifting buoys (hereafter called drifters) of the Global Drifter Program (Lumpkin & Pazos 2007) were analysed. This program is conducted by the US National Oceanic and Atmospheric Administration (NOAA). Drifters consist of a surface float equipped with a Global Positioning System (GPS) device, and a drogue centred at 15 m depth to ensure drifter movement along with ocean surface currents (Lumpkin & Pazos 2007). Interpolated data of all drifters passing 40–70°S 10–70°W between 15 February 1979 and 31 July 2007 were downloaded from http://www.aoml.noaa.gov/phod/dac/gdp.html. Three elliptical regions were defined to encompass the main shelf habitats of AP and South Shetland Islands, South Georgia, and South Sandwich Islands. Chosen diameters were 4° in latitudinal direction and 6° in longitudinal direction, which resulted in radii between 155 and 222 km, depending on latitude. Ellipses were centred at 61.84°S 56.33°W, 54.39°S 36.95°W, and 57.76°S 26.42°W, respectively. Drifter data was filtered to exclude all drifters that did not pass any of the three defined regions. To simulate dispersal of pelagic larvae from and to the shelf habitats, trajectories of the remaining drifters were plotted (i) over a period of 4 months, starting the day of departure from one of the regions, and (ii) for 4 months before arrival at one of the areas. The 4-month period was chosen to reflect the duration of the *G. gibberifrons* pelagic larval stage (North 2001). To account for potential surface current differences during the *G. gibberifrons* hatching period (North 2001), a third plot was produced using only drifters that left one of the regions between August and November.

Isolation-with-migration model

The isolation-with-migration (IM) model, as implemented in IMA (Hey & Nielsen 2007), was applied to determine directionality of gene flow between the AP shelf and the SR island shelves. To this end, all AP samples were grouped into one population, while South Georgia and South Sandwich Islands samples constituted the second population. Two possible scenarios of gene flow were considered: (i) unidirectional larval dispersal with ocean currents as approximated by drifter trajectories and (ii) bidirectional stepwise migration of adults along the SR. In both scenarios, we expected gene flow between South Georgia

and South Sandwich Islands to be direct, i.e. not via AP populations. For feasible run durations, the AP population was reduced to two independent subsets of 60 individuals each, drawn evenly from the four AP locations. Mitochondrial D-loop sequences and seven out of the eight microsatellite loci were included in the model. Trne35 was excluded, as null alleles were indicated by a departure from Hardy–Weinberg expectations, and TANDEM analysis revealed poor binning quality of this locus. To adjust for expected effective population sizes, inheritance scalars of 0.25 and 1 were assigned to mtDNA and microsatellite loci, respectively. The Hasegawa–Kishino–Yano (HKY) model of sequence evolution was applied to mitochondrial sequences, and a stepwise mutation model (SMM) was assumed for all microsatellite loci. Parameter ranges for uniform priors were empirically determined in a series of initial runs, and set to $m_1, m_2 \in (0,50]$, $t \in (0,10]$, and scalars $\Theta_1, \Theta_2, \Theta_A \in (0,3]$. Five final runs were conducted using both AP sample subsets. Each run included 40 Metropolis-coupled Markov chains and a geometric heating scheme. The first 1 million updates were discarded as burn-in. In each run, 100 000 genealogies were sampled from 10 million updates. Saved genealogies from all runs were combined according to AP subset for two subsequent analyses in IMA's 'Load-Trees' mode. Likelihood-ratio tests of nested models were conducted to assess whether unidirectional AP to SR gene flow can be rejected. Statistical significance was approximated using a chi-square (χ^2) distribution, following Hey & Nielsen (2007).

In order to exclude bias in gene flow directionality caused by unequal sample sizes, we ran an additional analysis with only 18 AP individuals to match the size of the combined SR population. AP individuals were drawn evenly from the four populations. In yet another approach to test for directionality bias, we used IMA to assess migration rates between sets of 18 and 60 individuals that were both drawn evenly from all AP populations, without inclusion of SR individuals. This was carried out three times, whereby the smaller subsets were non-overlapping between runs. For all runs, above settings for parameter ranges, number of Markov chains, heating scheme, and run duration were applied.

Results

Mitochondrial DNA: D-loop

Alignment of D-loop sequences from 162 individuals yielded a consensus sequence of 352 bp (GenBank Accession nos FJ528746–FJ528907). No gaps were found in the alignment. The ratio of transitions to transversions was 2.0. Sequences collapsed into 32 unique haplotypes (Table S2, Supporting information). DNA extraction, amplification and sequencing were repeated for 46 randomly chosen samples, confirming previous results. The resulting haplotype genealogy (Fig. 2) shows no obvious structure between populations.

Power analysis with POWSIM showed that the mtDNA data set had enough statistical power to detect global population structure with high probability when true F_{ST} values were as low as 0.02 (> 97%). With pooled AP and SR populations, this degree of divergence would be detected with a probability of 88% when using the χ^2 test (Fig. S1).

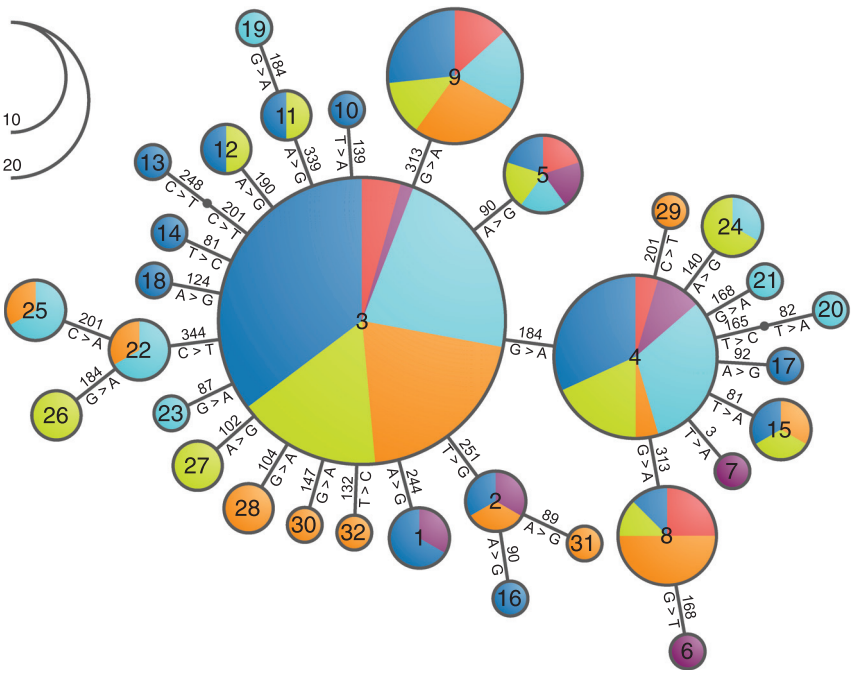

Fig. 2 Unrooted haplotype genealogy based on 162 D-loop sequences (352 bp). Radii reflect number of individuals.

Table 2 Population pairwise Φ_{ST} and F_{ST} values, based on mtDNA (below diagonal) and microsatellites (above diagonal) respectively. EI, Elephant Island; JIa, Joinville Island A; JIb, Joinville Island B; KGI, King George Island; SG, South Georgia; SSI, South Sandwich Islands

	EI	JIa	JIb	KGI	SG	SSI
Elephant Island		0.001	–0.001	0.001	0.001	–0.003
Joinville Island A	0.009		0.000	–0.001	0.000	–0.003
Joinville Island B	0.005	0.014		0.004	0.003	–0.004
King George Island	0.008	–0.017	0.011		0.005	0.001
South Georgia	0.042	–0.008	0.035	0.010		–0.009
South Sandwich Islands	0.058	0.029	–0.010	0.047	–0.001	

Of all possible groupings for the hierarchical AMOVA (Tables S3 and S4, Supporting information), the scheme with pooled AP populations and separate groups for SR populations produced high Φ_{ST} values relative to other groupings, and is therefore reported in more detail (Table S5, Supporting information). Here, 97% of variation occurred within populations, while only 2.5% and 0.4% were attributed to variation among groups and to variation within groups, but among populations. All Φ-statistics were low, and none were significant at the 95% confidence interval.

Population differentiation was further examined using pairwise comparisons (below diagonal in Table 2). Negative Φ_{ST} values are probably caused by rounding errors and are not significantly different from zero (Long 1986). The lowest Φ_{ST} values were found among the AP populations, while relatively higher fixation indices were detected between AP and SR populations. However, none of the pairwise Φ_{ST} values were significant at the 95% confidence level (below diagonal in Table S6, Supporting information).

Pairwise mutational distances were calculated over all 162 sequences and summarized in a coalescence-based mismatch analysis (Rogers & Harpending 1992). The model of sudden population expansion could not be rejected (sum of square deviation $P = 0.44$) (Fig. 3). As implemented in ARLEQUIN, the best-fitting model of population growth was calculated. The resulting model was characterized by expansion time parameter $\tau = 1.496$ (95% confidence interval: 1.199–1.961) and population size parameters $\Theta_0 = 0$ (0–0.098) and $\Theta_1 = 99\,999.0$ (6.871–99 999). Using a mutation rate of 6.5–8.8% per Myr and taking into account the sequence length of 352 bp, τ was translated to absolute time in years. Assuming this mutation rate applies for *Gobionotothen gibberifrons*, a sudden population expansion should have occurred 24 148–32 692 years before present (BP) (95% confidence interval: 19 353–42 854 BP).

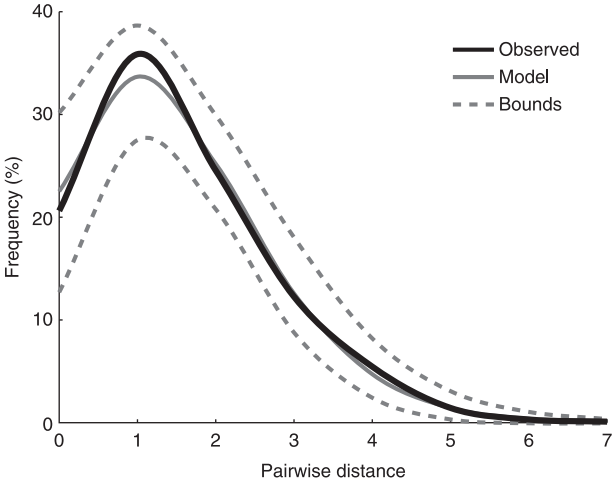

Fig. 3 Mismatch distribution over 162 *Gobionotothen gibberifrons* individuals, based on D-loop sequences (352 bp).

Nuclear DNA: microsatellites

A total of 164 individuals from six different sampling locations were scored for nine microsatellite loci. Analyses with TANDEM revealed effective repeat sizes between 1.83 and 2.15 bp, and average rounding errors between 0.04 and 0.38 bp. The largest average rounding error was associated with locus Trne35. The number of alleles per locus, allelic size range, as well as observed and expected heterozygosities are reported in Table S7, Supporting information. Up to 61 alleles were found for single loci. Locus Cr170 was monomorphic in all populations, as was Cr127 in all specimens from South Georgia. Trne35 featured the widest range of fragment sizes, and the largest number of alleles. However, for Trne35, the presence of null alleles was indicated by a significant ($P < 0.001$) departure from Hardy–Weinberg expectations (Table S7) in all AP populations (O'Connell & Wright 1997). Analysis with the software MICROCHECKER confirmed that null alleles are the causes of all departures from Hardy–Weinberg equilibrium. No tests for linkage disequilibrium were significant after Bonferroni correction (Rice 1989; Slatkin 1994; Slatkin & Excoffier 1996).

Statistical power analysis indicated high probabilities (> 99%) to detect global population structure when true F_{ST} values are as low as 0.005. Between AP and SR populations, the same degree of divergence would be detected with probabilities exceeding 92% and 98%, using Fisher's exact test and χ^2 test, respectively (Fig. S2).

Hierarchical AMOVA tests indicated that almost all variation (~100%) occurred within populations. Hardly any genetic differentiation was attributed to population or group identities, irrespective or grouping scheme (Table S8, Supporting information). Detailed results are reported for the grouping chosen for mtDNA sequences in Table S9, Supporting information.

Applying *F*-statistics to the same microsatellite data set confirmed genetic homogeneity between populations (above diagonal in Table 2). F_{ST} values range between –0.009 and 0.005. Given that the greatest absolute value and the average F_{ST} were negative, it is likely that rounding errors are responsible for all departures from zero. None of the associated *p*-values (above diagonal in Table S6) were significant after Bonferroni correction.

Above findings were corroborated by the clustering method implemented in STRUCTURE. Log-likelihood values were calculated for the existence of $1 \leq K \leq 6$ clusters within the microsatellite data set. The highest log-likelihood value was scored for the assignment of all individuals to a single cluster ($K = 1$) in three independent run replicates. Log-likelihood values decreased with increasing number of assumed clusters (Table S10, Supporting information).

Drifter analysis

A total of 661 drifters crossed 40–70°S latitude and 10–70°W longitude between 15 February 1979 and 31 July 2007, and 140 of them entered one of the predefined areas around the AP and SR populations. Out of 52 drifters that left the AP shelf area, 13 drifters reached South Georgia within four months. Of those leaving the South Georgia or South Sandwich Island areas (21 and 8 drifters, respectively), none arrived at a different area within the 4-month period (Fig. 4A).

When including only drifters that left during the *G. gibberifrons* hatching period between August and November (North 2001), a similar picture arises. A single drifter left the AP area within this period and arrived at the South Georgia area after three and a half months. To the contrary, five drifters were advected off the South Georgia shelf, and dispersed into the Southwest Atlantic without crossing other shelf areas (Fig. 4B). A multivariate analysis of variation (MANOVA) was run to compare trajectory endpoints of drifters that left the South Georgia shelf between August and November with those of drifters leaving between December and July (R Development Core Team 2008). No significant difference was found ($F_{2,18} = 1.89$, $P = 0.18$). Thus, using year-round drifters as proxies for *G. gibberifrons* larval dispersal seems reasonable.

Finally, we analysed drifter histories over 4 months prior to entrance of predefined shelf areas. Three drifters entered the AP area from the west; none of them had come close to other areas. Out of 25 drifters that entered the South Georgia area, one had left the AP shelf area 4 months earlier, and several more passed this area within short distance. A single drifter entered the South Sandwich Islands area coming from South Georgia (Fig. 4C).

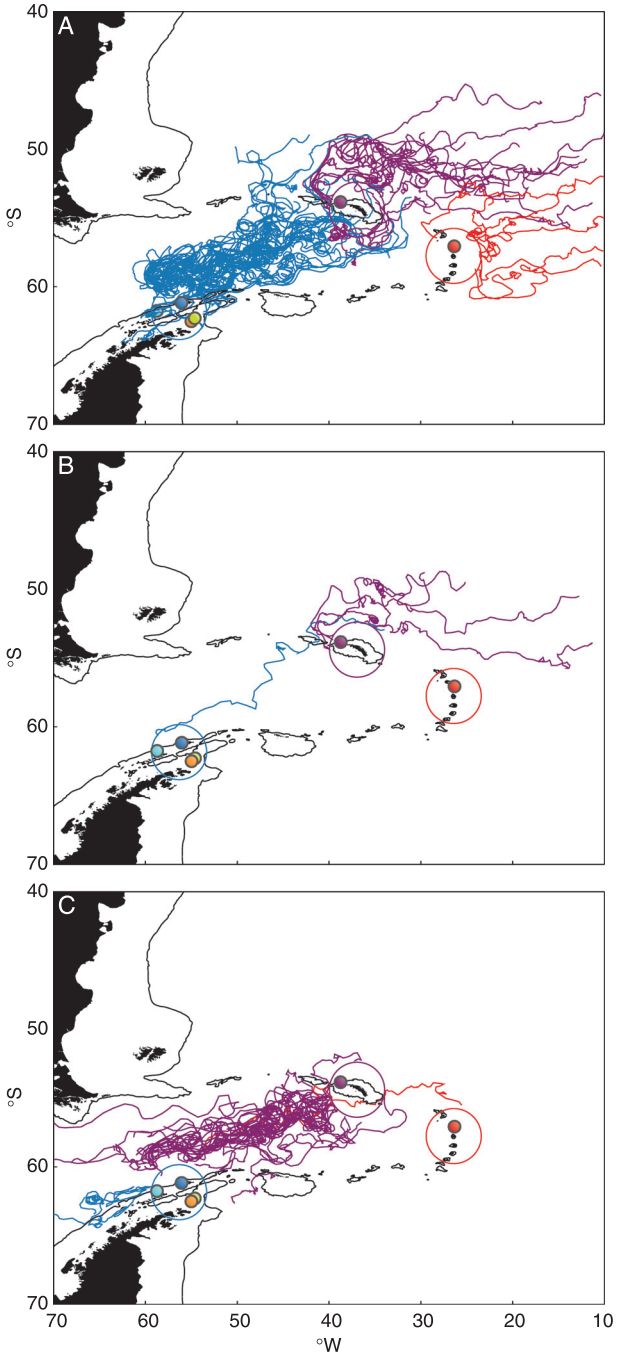

Fig. 4 Trajectories of Surface Velocity Program Drifters in the Scotia Sea and the Southwest Atlantic between 1979 and 2007. (A) Four-month drifter trajectories after departure from shelf areas approximated by three elliptical regions. (B) As in (A), but using only drifters that left one of the regions between August and November. (C) Four-month drifter trajectories before entering one of the three regions.

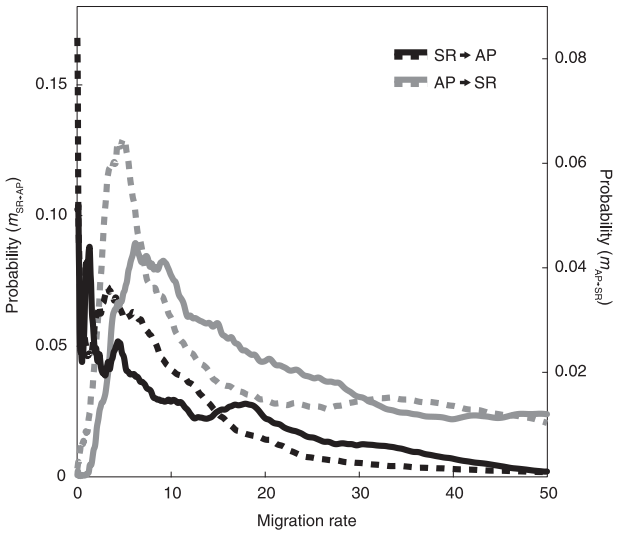

Fig. 5 Posterior probabilities of migration rates determined with IMA. Black: SR to AP migration rates, grey: AP to SR migration rates. Solid line: using the first AP subset of 60 *Gobionotothen gibberifrons* individuals, dashed line: using the second AP subset.

Isolation-with-migration model

Our aim was to discriminate between two contrasting scenarios of gene flow across the Scotia Sea: bidirectional adult migration or unidirectional larval dispersal from the AP to the SR. Replicate runs of the IMA program revealed asymmetric migration rates (Fig. 5). In two independent sample subsets, the highest posterior probabilities for SR to AP migration rates (scaled for mutation rate) were consistently found close to zero (0.025 and 0.075). Out of 1000 bins distributed evenly over the whole parameter range, these values corresponded to the two bins closest to zero. On the other hand, nonzero rates were inferred for AP to SR migration (4.875 and 6.225). One of two sample subsets produced sharp peaks for all three population size parameters (Θ_1: 27.166, Θ_2: 24.476, Θ_A: 79.007). The second subset failed to produce a clear peak for the SR population size parameter, but AP and ancient population size parameters were congruent with the first subset (Θ_1: 30.470, Θ_A: 87.763). Population size parameters of the first subset were used to convert migration parameters into per-generation population migration rates ($M = \Theta \times m/2$). Peak locations corresponded to 59.659 and 76.180 migration events per generation. Taking into account a *G. gibberifrons* generation time of 6–8 years (Kock & Kellermann 1991), this translates to 7.45–12.70 migration events per year. Likelihood ratio tests did not reject unidirectional AP to SR gene flow in either subset ($P_1 = 0.19$, $P_2 = 0.23$), whereas unidirectional gene flow in the opposite direction, from the SR to the AP, was clearly rejected in one out of two subsets ($P_1 = 0.18$, $P_2 < 0.0001$).

In order to test for directionality bias, we used IMA to estimate migration rates (i) between equally sized sets of 18 AP and 18 SR individuals, and (ii) between sets of 60 and 18 individuals that were both drawn evenly from all AP populations. In the first case, reduction of the AP sample size did not influence directionality of migration rates. The highest posterior probability was assigned to a near-zero SR to AP migration rate (0.025), while a substantially higher rate was found in the opposite direction (3.225). In the second case of unequal sample sizes, we found mostly balanced gene flow between the larger and the smaller subset of AP individuals (m_1: 4.475, 7.075, 0.925; m_2: 5.625, 4.225, 6.325; all values scaled for mutation rate). These results suggest that estimation of migration rates, as implemented in IMA, is robust to unequal sample sizes. Taken together, our analyses using the IM model indicate unidirectional gene flow across the Scotia Sea, from the AP shelf to South Georgia and the South Sandwich Islands.

Discussion

Demographic history of Gobionotothen gibberifrons

We investigated the demographic history of the total *Gobionotothen gibberifrons* population using a coalescent-based mismatch analysis, as implemented in ARLEQUIN. In order to date the observed sudden population expansion, we assumed a control region mutation rate of 6.5–8.8% per Myr that has been found in Lake Malawi cichlid fishes, another perciform group that underwent adaptive radiation (Sturmbauer *et al*. 2001). Applying this rate, our results suggest an expansion 24 148–32 692 years ago, at the height of the last ice age (EPICA community members 2004). Presumably, the Antarctic ice sheet extended all the way to the shelf in glacial cycles (Thatje *et al*. 2008), 'bulldozing the surviving fauna to the deep continental margin' (Barnes & Conlan 2007). It seems difficult to imagine how extensive glaciation of the Antarctic shelf, the *G. gibberifrons* habitat, may have contributed to increasing population size. However, time estimates based on molecular clocks should in general be treated with caution, and serve as rough approximations only. Published estimates of control region mutation rates in bony fishes vary on two orders of magnitude. For example, mutation rates as low as 2.2% per Myr were inferred for haplochromine cichlids (Sato *et al*. 2003), while rates up to 108% per Myr were estimated for Indo-Pacific butterflyfishes (McMillan & Palumbi 1997; see Bowen *et al*. 2006 for a list of published estimates). It has recently been shown that variation in mitochondrial mutation rates can partly be explained by metabolic rate and generation time (Nabholz *et al*. 2008). The metabolic rate hypothesis states that the mitochondrial mutation rate is linked to metabolic rate and production of reactive oxygen species (ROS) (Martin & Palumbi 1993, but see Lanfear

et al. 2007). Given the low metabolic rate of notothenioids (Clarke & Johnston 1999), a low mutation rate could be expected (Bargelloni *et al*. 1994). In addition, the generation time of *G. gibberifrons* (6–8 years, Kock & Kellermann 1991) is higher than in cichlid fishes (1–3 years, Won *et al*. 2005). Therefore, the assumed mutation rate of 6.5–8.8% could be an overestimate, and the population expansion might be older than inferred. Should the *G. gibberifrons* substitution rate be substantially lower, the expansion could date back to the beginning of the last interglacial 180 000 years ago (EPICA community members 2004) when the Antarctic ice sheet disconnected from the shelf floor, and suitable shelf habitat became available. On the other hand, most Antarctic notothenioids lack NADH 6 dehydrogenase, which is part of the mitochondrial electron transport chain. It has been hypothesized that this loss allows heat production through proton leakage across the inner mitochondrial membrane (Papetti *et al*. 2007a). If so, possible consequences on ROS production, and thus on mutation rate, cannot be excluded. Unusually high mutation rates of the mitochondrial control region have previously been observed in butterflyfishes (McMillan & Palumbi 1997; 33–108%). Of interesting note, very similar shapes of mismatch distributions have been found in another Antarctic notothenioid, *Pleuragramma antarcticum*, as well as in Antarctic krill, *Euphausia superba* Dana (Zane *et al*. 2006, 1998). Taken together, these findings suggest that periodical glaciations may have affected a large part of the Antarctic marine fauna in one way or another. However, more precise estimates of notothenioid mutation rates will be needed in order to correlate demographic histories of different species, and to shed light on potential geological and/or climatological causes of population expansions.

Larval dispersal across the Scotia Sea

Our genetic analyses based on neutral mitochondrial and nuclear markers show no significant population structure between *G. gibberifrons* populations around the Scotia Sea suggesting ongoing gene flow between sampling sites. Between-population fixation indices were close to zero and AMOVA tests attributed ~100% of genetic differentiation to variation within populations. Although genetic homogeneity could theoretically be explained solely by ancestral polymorphism, our analyses using the isolation-with-migration model confirm that large amounts of gene flow do occur between *G. gibberifrons* populations. Moreover, our results suggest that gene flow is highly unidirectional, following the direction of the ACC. However, our results may be affected by departures from the strict IM model. Since this model only considers pairs of populations, estimates of migration rates can be distorted by unsampled populations that exchange migrants with the two sampled populations (Won & Hey 2005). In the Scotia Sea, the shelf area surrounding the South Orkney Islands harbours a large *G. gibberifrons* population (Kock & Jones 2005). Given its geographic location between the AP and SR sampling locations, it seems possible that gene flow between the AP and the SR sampling locations occurs via the South Orkney shelf. The effect of so-called 'ghost populations' is difficult, if not impossible to quantify, in particular if migration is asymmetric (Slatkin 2005). Furthermore, population subdivisions would violate the IM model and affect migration rate estimates (Wakeley 2000). However, given our above results of mtDNA and microsatellite data, we consider both AP and SR populations as panmictic, and thus in agreement with the model. Based on additional analyses using equally sized AP and SR subsets as well as AP subsets of different sizes, we conclude that unequal sample sizes apparently do not affect migration rate estimates of the IMA program. Similar results were found for the software IM, that implements the same model and is structurally related to IMA (Hey & Nielsen 2004; Rosenblum 2006). Taken together, we found a clear signal of unidirectional gene flow that is not affected by unequal sample sizes, and thus must be inherent to the data.

Analyses of surface drifter trajectories show that passive particles cross the Scotia Sea between AP and South Georgia in less than 4 months, the pelagic larval duration of *G. gibberifrons*. We therefore conclude that larval dispersal along the ACC is the main agent of gene flow in *G. gibberifrons*. Given the extended pelagic phases of many notothenioid fishes, larval dispersal with the ACC has been suggested for a number of notothenioid species (Loeb *et al*. 1993). In a recent survey of the ichthyofauna of Bouvetøya, a small volcanic island within the ACC, about 2500 km east of South Georgia, all detected nototheniid and channichthyid species had long larval durations of 1–2 years (Jones *et al*. 2008). In contrast to similarly isolated islands (e.g. Easter Island), not a single endemic fish species was found at Bouvetøya. Jones *et al*. (2008) conclude that the Bouvetøya ichthyofauna is primarily derived from South Georgia, through dispersal of pelagic larvae with the ACC.

Marine populations have long been considered demographically open, and generally interconnected by larval dispersal. It was believed that virtually all fish larvae would be advected from the local sources to settle in downstream habitats (Caley *et al*. 1996). However, this view has shifted in recent years as evidence for larval retention has accumulated (reviewed in Swearer *et al*. 2002). Many larvae are capable of active vertical migration, which in combination with vertically stratified flows may suffice to avoid advection, and especially towards the end of their pelagic phase, larvae are able to swim even faster than ambient currents in many cases (Leis 2006). In notothenioids, larvae of many species, including *G. gibberifrons*, are known to undergo vertical migration (North & Murray 1992). Thus, active retention mechanisms could potentially counteract advection with the

Table 3 Summary of published studies on the population structure of notothenioids. These include studies employing allozyme electrophoresis (the number of analysed protein-coding loci is given), restriction fragment length polymorphisms (RFLP, number of informative restriction enzymes), randomly amplified polymorphic DNA (RAPD, number of polymorphic primers), mitochondrial (mtDNA) and nuclear DNA (nDNA) sequence analysis (fragment length is given) and microsatellite analysis (STR, number of polymorphic loci). The shortest distance over which significant differentiation was found (d_s) is given, as well as the longest distance over which no significant divergence could be detected (d_{ns}). *Nonsignificant differentiation within the Weddel Sea. †Details not reported in publication. ‡Differentiation found between collections of different years

Organism	*N*	Allozymes	RFLP	RAPD	mtDNA	nDNA	STR	d_s (km)	d_{ns} (km)	Reference
Champsocephalus gunnari	53		7					—	400	Williams *et al*. (1994)
Lepidonotothen squamifrons	215	5						6400	1300	Schneppenheim *et al*. (1994)
Champsocephalus gunnari	86	13						—	6400	Duhamel *et al*. (1995)
Notothenia rossii	76	13						—	400	Duhamel *et al*. (1995)
Chionodraco myersi	65	10						16	< 1000*	Clement *et al*. (1998)
Neopagetopsis ionah	35	10						4600	< 1000*	Clement *et al*. (1998)
Dissostichus eleginoides	32						5	60	—	Reilly & Ward (1999)
Dissostichus eleginoides	196–230	7					8	2000	6000	Smith & McVeagh (2000)
Dissostichus eleginoides	? †	?			?		?	~500	8300	Smith & Gaffney (2000)
Dissostichus eleginoides	439–623		2				7	5200	—	Appleyard *et al*. (2002)
Dissostichus mawsoni	42			12				4700	—	Parker *et al*. (2002)
Chionodraco hamatus	74				302 bp			1000	9300	Patarnello *et al*. (2003)
Dissostichus eleginoides	113–136		2				7	—	2600	Appleyard *et al*. (2004)
Dissostichus eleginoides	396–450		2				5	500	1300	Shaw *et al*. (2004)
Dissostichus mawsoni	24–57		4		1304 bp		5	—	5000	Smith & Gaffney (2005)
Champsocephalus gunnari	63				1817 bp	3037 bp		1200	4400	Kuhn & Gaffney (2006)
Dissostichus eleginoides	151–274				249 bp		7	1200	5100	Rogers *et al*. (2006)
Pleuragramma antarcticum	256				277 bp			0‡	7000	Zane *et al*. (2006)
Trematomus bernacchii	61				468 bp	307 bp		4900	1600	Janko *et al*. (2007)
Trematomus newnesi	36				483 bp	299 bp		—	4900	Janko *et al*. (2007)
Chaenocephalus aceratus	247						11	—	100	Papetti *et al*. (2007b)
Dissostichus mawsoni	4–68				~4000 bp	~11 500 bp		1300	7800	Kuhn & Gaffney (2008)
Chaenocephalus aceratus	23				1047 bp			—	3900	Jones *et al*. (2008)
Lepidonotothen squamifrons	23				1047 bp			3400	1800	Jones *et al*. (2008)
Notothenia coriiceps	21				1047 bp			—	3900	Jones *et al*. (2008)
Lepidonotothen larseni	23				1047 bp			—	3400	Jones *et al*. (2008)
G. gibberifrons	162–164				352 bp		8	—	1900	This study

ACC. At South Georgia, off-shelf dispersal was observed for pelagic fish eggs, but not for notothenioid larvae, suggesting active larval behaviour (White 1998). On the other hand, Kellermann (1991) found larvae of *Notothenia coriiceps*, another benthic nototheniid, at a number of Scotia Sea sampling locations between the AP and South Georgia shelves. Moreover, positive catches occurred earlier in the southern Scotia Sea than near South Georgia, leading Kellermann (1991) to conclude that larvae hatched near the AP and reach South Georgia with the ACC. Less is known about the distribution of *G. gibberifrons* larvae. However, large numbers of larvae were occasionally found in offshore waters around South Georgia (Loeb *et al*. 1993). These observations corroborate our results, showing that advection of notothenioid larvae away from their local shelf habitats does indeed occur, and that larvae can travel hundreds of kilometres, surfing the ACC. In *G. gibberifrons*, we detected no significant population structure across distances as large as 1900 km, comprising a large part of the species' distribution range (Fig. 1). These results are comparable to findings of previous studies on genetic differentiation in notothenioids (Table 3).

Our analyses based on the IM model suggest around 10 migration events per year between the AP and the SR populations of South Georgia and the South Sandwich Islands. In order to calculate per-generation migration rates, we used the equation $M = \Theta \times m/2$, which assumes genetic equilibrium of populations. We note that this cannot be the case for *G. gibberifrons*, as we detected a recent population expansion. Therefore, the detected number of migration events should be treated as a rough estimate. However, to maintain genetic homogeneity between populations, even lower rates would be sufficient (Slatkin 1987). As the population size of *G. gibberifrons* is large (Kock & Jones 2005), detected migration rates are negligible for demographic processes. This would mean that most of

the South Georgia population recruits locally. It remains unclear, whether this is due to active retention mechanisms, mortality of advected larvae, or low mating success of migrants. But over time periods important for evolutionary processes, AP populations represent source populations, while SR populations constitute sinks. Travelling with the ACC, larvae advected from SR shelves would fail to find suitable habitat. Given this risk of losses due to advection, the presence of extended pelagic larval phases in many Antarctic fishes (1–2 years, Loeb *et al*. 1993) seems puzzling, but may be balanced by retention mechanisms (White 1998) that save most larvae from advection. Although highly speculative, protracted larval phases might be explained by selection for dispersal subsequent to range expansions (Thomas *et al*. 2001). As mentioned above, many shelf habitats close to the Antarctic continent were covered by the Antarctic ice cap during ice ages. Following glacial retreat, habitats became available and presumably caused range expansions, whereby longer larval phases could have been favoured.

Overall, our results compare well with those of similar studies. Table 3 summarizes, to the best of our knowledge, all published population genetic studies of notothenioid fishes. Despite large variation in sample size and markers used, nonsignificant differentiation is commonly found across thousands of kilometres (d_{ns}) and even between populations at opposite sides of Antarctica (Patarnello *et al*. 2003). Significant differentiation over less than 100 km was found only in very few cases. Of particular note are findings on the population structure of *Chionodraco myersi*, a benthic channichthyid (Iwami & Kock 1990) with long pelagic larval phase (Kock & Kellermann 1991), and *P. antarcticum*, one of few notothenioids that adapted a truly pelagic lifestyle (Eastman 1993). Using allozyme markers, Clement *et al*. (1998) detected significant differentiation between *C. myersi* Weddel Sea populations no more than 16 km apart. The authors attribute this differentiation to a rapid geotrophic stream running between both populations. Perhaps more surprising were findings in *P. antarcticum*. Using comparatively large sample sizes and mitochondrial control region sequences, Zane *et al*. (2006) found significant differentiation between samples taken at Halley Bay, Weddell Sea at intervals of 2 years, but no significant differentiation between samples taken on opposite sides of the continent. These exceptions aside, it seems that gene flow across large distances is a common feature in notothenioids.

Acknowledgements

We thank Reiner Eckmann and Moritz Muschick for discussion, Markus Busch, Sven Klimpel, Karl-Hermann Kock and Christopher Jones for sampling support, Frauke Münzel for assistance in DNA extractions, Daniel Berner for assistance using R, and Adolf Kellermann for valuable suggestions based on his unpublished data. We also thank the subject editor Michael Hansen, and three anonymous reviewers for comments on the manuscript. This study was supported by a PhD scholarship of the VolkswagenStiftung priority program 'Evolutionary Biology' for M.M., a grant from the German Research Foundation (DFG) to R.H., and funding from the European Research Council (ERC; Starting Grant 'INTERGENADAPT') to W.S.

References

Appleyard SA, Ward RD, Williams R (2002) Population structure of the Patagonian toothfish around Heard, McDonald and Macquarie Islands. *Antarctic Science*, **14**, 364–373.

Appleyard SA, Williams R, Ward RD (2004) Population genetic structure of Patagonian toothfish in the West Indian sector of the Southern Ocean. *CCAMLR Science*, **11**, 12–32.

Bargelloni L, Ritchie PA, Patarnello T *et al*. (1994) Molecular evolution at subzero temperatures: mitochondrial and nuclear phylogenies of fishes from Antarctica (suborder Notothenioidei), and the evolution of antifreeze glycopeptides. *Molecular Biology and Evolution*, **11**, 854–863.

Barnes DKA, Conlan KE (2007) Disturbance, colonization and development of Antarctic benthic communities. *Philosophical Transactions of the Royal Society B: Biological Sciences*, **362**, 11–38.

Barnes DKA, Fuentes V, Clarke A, Schloss IR, Wallace MI (2006) Spatial and temporal variation in shallow seawater temperatures around Antarctica. *Deep Sea Research Part II: Topical Studies in Oceanography*, **53**, 853–865.

Bowen BW, Muss A, Rocha LA, Grant WS (2006) Shallow mtDNA coalescence in Atlantic pygmy angelfishes (genus *Centropyge*) indicates a recent invasion from the Indian Ocean. *Journal of Heredity*, **97**, 1–12.

Brunner PC, Douglas MR, Osinov A, Wilson CC, Bernatchez L (2001) Holarctic phylogeography of Arctic charr (*Salvelinus alpinus* L.) inferred from mitochondrial DNA sequences. *Evolution*, **53**, 573–586.

Caley MJ, Carr MH, Hixon MA *et al*. (1996) Recruitment and the local dynamics of open marine populations. *Annual Review of Ecology and Systematics*, **27**, 477–500.

Chen L, DeVries AL, Cheng CHC (1997) Evolution of antifreeze glycoprotein gene from a trypsinogen gene in Antarctic notothenioid fish. *Proceedings of the National Academy of Sciences, USA*, **94**, 3811–3816.

Clarke A, Johnston NM (1999) Scaling of metabolic rate with body mass and temperature in teleost fish. *Journal of Animal Ecology*, **68**, 893–905.

Clement O, Ozouf-Costaz C, Lecointre G, Berrebi P (1998) Allozymic polymorphism and phylogeny of the family Channichthyidae. In: *Fishes of Antarctica. A Biological Overview* (eds di Prisco G, Pisano E, Clarke A), pp. 299–309. Springer-Verlag Publishers, Milan, Italy.

Cziko PA, Cheng CHC (2006) A new species of notothenid (Perciformes: Notothenioidei) fish from McMurdo Sound, Antarctica. *Copeia*, **2006**, 752–759.

Derome N, Chen WJ, Dettaï A, Bonillo C, Lecointre G (2002) Phylogeny of Antarctic dragonfishes (Bathydraconidae, Notothenioidei, Teleostei) and related families based on their anatomy and two mitochondrial genes. *Molecular Phylogenetics and Evolution*, **24**, 139–152.

DeVries AL (1988) The role of antifreeze glycopeptides and peptides in the freezing avoidance of Antarctic fishes. *Comparative Biochemistry and Physiology*, **90B**, 611–621.

DeWitt HH, Heemstra PC, Gon O (1990) Nototheniidae. In: *Fishes of the Southern Ocean* (eds Gon O, Heemstra PC), pp. 279–332 J.L.B. Smith Institute of Ichthyology, Grahamstown, South Africa.

Domingues VS, Bucciarelli G, Almada VC, Bernardi G (2005) Historical colonization and demography of the Mediterranean damselfish, *Chromis chromis*. *Molecular Ecology*, **14**, 4051–4063.

Duhamel G, Ozouf-Costaz C, Cattaneo-Berrebi G, Berrebi P (1995) Interpopulation relationships in two species of Antarctic fish *Notothenia rossii* and *Champsocephalus gunnari* from the Kerguelen Islands: an allozyme study. *Antarctic Science*, **7**, 351–356.

Eastman JT (1993) *Antarctic Fish Biology: Evolution in a Unique Environment*. Academic Press, San Diego, California.

Eastman JT (2005) The nature of the diversity of Antarctic fishes. *Polar Biology*, **28**, 93–107.

Eastman JT, Clarke A (1998) A comparison of adaptive radiations of Antarctic fish with those of non-Antarctic fish. In: *Fishes of Antarctica. A Biological Overview* (eds di Prisco G, Pisano E, Clarke A), pp. 3–26. Springer-Verlag Publishers, Milan, Italy.

EPICA community members (2004) Eight glacial cycles from an Antarctic ice core. *Nature*, **429**, 623–628.

Excoffier L, Laval G, Schneider S (2005) ARLEQUIN version 3.0: an integrated software package for population genetics data analysis. *Evolutionary Bioinformatics Online*, **1**, 47–50.

Falush D, Stephens M, Pritchard JK (2007) Inference of population structure using multilocus genotype data: dominant markers and null alleles. *Molecular Ecology Notes*, **7**, 574–578.

Foster TD (1984) The marine environment. In: *Antarctic Ecology* (ed. Laws RM) **2**, pp. 345–371. Academic Press, London.

Hasegawa M, Kishino H, Yano T (1985) Dating of the human–ape splitting by a molecular clock of mitochondrial DNA. *Journal of Molecular Evolution*, **22**, 160–174.

Hey J, Nielsen R (2004) Multilocus methods for estimating population sizes, migration rates and divergence time, with applications to the divergence of *Drosophila pseudoobscura* and *D. persimilis*. *Genetics*, **167**, 747–760.

Hey J, Nielsen R (2007) Integration within the Felsenstein equation for improved Markov chain Monte Carlo methods in population genetics. *Proceedings of the National Academy of Sciences, USA*, **104**, 2785–2790.

Iwami T, Kock KH (1990) Channichthyidae. In: *Fishes of the Southern Ocean* (eds Gon O, Heemstra PC), pp. 279–332 J.L.B. Smith Institute of Ichthyology, Grahamstown, South Africa.

Janko K, Lecointre G, DeVries AL *et al*. (2007) Did glacial advances during the Pleistocene influence differently the demographic histories of benthic and pelagic Antarctic shelf fishes? — Inferences from intraspecific mitochondrial and nuclear DNA sequence diversity. *BMC Evolutionary Biology*, **7**, 220–220.

Jones CD, Anderson ME, Balushkin AV *et al*. (2008) Diversity, relative abundance, new locality records and population structure of Antarctic demersal fishes from the northern Scotia Arc islands and Bouvetøya. *Polar Biology*, **31**, 1481–1497.

Kellermann AK (1991) Egg and larval drift of the Antarctic fish *Notothenia coriiceps*. *Cybium*, **15**, 199–210.

Kock KH (1992) *Antarctic Fish and Fisheries*. Cambridge University Press, Cambridge, UK.

Kock KH (2005) Antarctic icefishes (Channichthyidae): a unique family of fishes. A review, part I. *Polar Biology*, **28**, 862–895.

Kock KH, Jones CD (2005) Fish stocks in the Southern Scotia Arc region — a review and prospects for future research. *Reviews in Fisheries Science*, **13**, 75–108.

Kock KH, Kellermann AK (1991) Reproduction in Antarctic notothenioid fish. *Antarctic Science*, **3**, 125–150.

Kompowski A (1985) Studies on food and fecundity of *Notothenia gibberifrons* Lönnberg, 1905 (Pisces, Notothenioidei) off South Georgia. *Acta Ichthyologica et Piscatoria*, **15**, 55–73.

Kuhn KL, Gaffney PM (2006) Preliminary assessment of population structure in the mackerel icefish (*Champsocephalus gunnari*). *Polar Biology*, **29**, 927–935.

Kuhn KL, Gaffney PM (2008) Population subdivision in the Antarctic toothfish (*Dissostichus mawsoni*) revealed by mitochondrial and nuclear single nucleotide polymorphisms (SNPs). *Antarctic Science*, **20**, 12.

Lanfear R, Thomas JA, Welch JJ, Brey T, Bromham L (2007) Metabolic rate does not calibrate the molecular clock. *Proceedings of the National Academy of Sciences, USA*, **104**, 15388–15393.

Leis JM (2006) Are larvae of demersal fishes plankton or nekton? *Advances in Marine Biology*, **51**, 57–141.

Li WH (1977) Distribution of nucleotide differences between two randomly chosen cistrons in a finite population. *Genetics*, **85**, 331–337.

Loeb VJ, Kellermann AK, Koubbi P, North AW, White MG (1993) Antarctic larval fish assemblages: a review. *Bulletin of Marine Science*, **53**, 416–449.

Long JC (1986) The allelic correlation structure of Gainj- and Kalam-speaking people. I. the estimation and interpretation of Wright's *F*-statistics. *Genetics*, **112**, 629–647.

Lumpkin R, Pazos M (2007) Measuring surface currents with surface velocity program drifters: the instrument, the data, and some recent results. In: *Lagrangian Analysis and Prediction of Coastal and Ocean Dynamics* (eds Mariano A, Rossby T, Kirwan D), pp. 39–67. Cambridge University Press, Cambridge, UK.

Martin AP, Palumbi SR (1993) Body size, metabolic rate, generation time, and the molecular clock. *Proceedings of the National Academy of Sciences, USA*, **90**, 4087–4091.

Matschiner M, Salzburger W (2009) TANDEM: integrating automated allele binning into genetics and genomics workflows. *Bioinformatics*, [Epub ahead of print] doi: 10.1093/bioinformatics/btp303.

Mayr E (1984) Evolution of fish species flocks: a commentary. In: *Evolution of Fish Species Flocks* (eds Echelle AT, Kornfield A), pp. 3–12. University of Maine at Orono Press, Orono, Maine.

McMillan WO, Palumbi SR (1997) Rapid rate of control-region evolution in Pacific butterflyfishes (Chaetodontidae). *Journal of Molecular Evolution*, **45**, 473–484.

Nabholz B, Glemin S, Galtier N (2008) Strong variations of mitochondrial mutation rate across mammals — the longevity hypothesis. *Molecular Biology and Evolution*, **25**, 120–130.

North AW (2001) Early life history strategies of notothenioids at South Georgia. *Journal of Fish Biology*, **58**, 496–505.

North AW, Murray AWA (1992) Abundance and diurnal vertical distribution of fish larvae in early spring and summer in a fjord at South Georgia. *Antarctic Science*, **4**, 405–412.

O'Connell M, Wright JM (1997) Microsatellite DNA in fishes. *Reviews in Fish Biology and Fisheries*, **7**, 331–363.

Papetti C, Zane L, Patarnello T (2006) Isolation and characterization of microsatellite loci in the icefish *Chionodraco rastrospinosus* (Perciformes, Notothenioidea, Channichthyidae). *Molecular Ecology Notes*, **6**, 207–209.

Papetti C, Liò P, Rüber L, Patarnello T, Zardoya R (2007a) Antarctic fish mitochondrial genomes lack ND6 gene. *Journal of Molecular Evolution*, **65**, 519–528.

Papetti C, Susana E, Mesa ML *et al*. (2007b) Microsatellite analysis reveals genetic differentiation between year-classes in the icefish *Chaenocephalus aceratus* at South Shetlands and Elephant Island. *Polar Biology*, **30**, 1605–1613.

Parker RW, Paige KN, DeVries AL (2002) Genetic variation among populations of the Antarctic toothfish: evolutionary insights and implications for conservation. *Polar Biology*, **25**, 256–261.

Patarnello T, Marcato S, Zane L, Varotto V, Bargelloni L (2003) Phylogeography of the *Chionodraco* genus (Perciformes, Channichthydae) in the Southern Ocean. *Molecular Phylogenetics and Evolution*, **28**, 420–429.

Posada D, Crandall KA (1998) MODELTEST: testing the model of DNA substitution. *Bioinformatics*, **14**, 817–818.

Puebla O, Bermingham E, Guichard F (2008) Population genetic analyses of *Hypoplectrus* coral reef fishes provide evidence that local processes are operating during the early stages of marine adaptive radiations. *Molecular Ecology*, **17**, 1405–1415.

R Development Core Team (2008) *R: A Language and Environment for Statistical Computing*. R Foundation for Statistical Computing, Vienna, Austria. ISBN 3-900051-07-0. www. R-project.org.

Reilly A, Ward RD (1999) Microsatellite loci to determine population structure of the Patagonian toothfish *Dissostichus eleginoides*. *Molecular Ecology*, **8**, 1753–1754.

Rice WR (1989) Analysing tables of statistical tests. *Evolution*, **43**, 223–225.

Rico C, Turner GF (2002) Extreme microallopatric divergence in a cichlid species from Lake Malawi. *Molecular Ecology*, **11**, 1585–1590.

Rogers AR, Harpending H (1992) Population growth makes waves in the distribution of pairwise genetic differences. *Molecular Biology and Evolution*, **9**, 552–569.

Rogers AD, Morley S, Fitzcharles E, Jarvis K, Belchier M (2006) Genetic structure of Patagonian toothfish (*Dissostichus eleginoides*) populations on the Patagonian Shelf and Atlantic and western Indian Ocean Sectors of the Southern Ocean. *Marine Biology*, **149**, 915–924.

Rosenblum EB (2006) Convergent evolution and divergent selection: lizards at the white sands ecotone. *The American Naturalist*, **167**, 1–15.

Ryman N, Palm S (2006) POWSIM: a computer program for assessing statistical power when testing for genetic differentiation. *Molecular Ecology Notes*, **6**, 600–602.

Salzburger W (2008) To be or not to be a hamlet pair in sympatry. *Molecular Ecology*, **17**, 1397–1399.

Salzburger W (2009) The interaction of sexually and naturally selected traits in the adaptive radiations of cichlid fishes. *Molecular Ecology*, **18**, 169–185.

Sato A, Takezaki N, Tichy H *et al*. (2003) Origin and speciation of haplochromine fishes in East African crater lakes investigated by the analysis of their mtDNA, Mhc genes, and SINEs. *Molecular Biology and Evolution*, **20**, 1448–1462.

Schluter D (2000) *The Ecology of Adaptive Radiation*. Oxford University Press, New York.

Schneppenheim R, Kock KH, Duhamel G, Janssen G (1994) On the taxonomy of the *Lepidonotothen squamifrons* group (Pisces, Perciformes, Notothenioidei). *Archive of Fishery and Marine Research*, **42**, 137–148.

Shaw PW, Arkhipkin A, Al-Khairulla H (2004) Genetic structuring of Patagonian toothfish populations in the Southwest Atlantic Ocean: the effect of the Antarctic Polar Front and deep-water troughs as barriers to genetic exchange. *Molecular Ecology*, **13**, 3293–3303.

Sidell BD, O'Brien K (2006) When bad things happen to good fish: the loss of hemoglobin and myoglobin expression in Antarctic icefishes. *The Journal of Experimental Biology*, **209**, 1791–1802.

Silva S. N, Helbling EW, Villafañe VE, Amos AF, Holm-Hansen O (1995) Variability in nutrient concentrations around Elephant Island, Antarctica, during 1991–93. *Polar Research*, **14**, 69–82.

Slatkin M (1987) Gene flow and the geographic structure of natural populations. *Science*, **236**, 787–792.

Slatkin M (1994) Linkage disequilibrium in growing and stable populations. *Genetics*, **137**, 331–336.

Slatkin M (2005) Seeing ghosts: the effect of unsampled populations on migration rates estimated for sampled populations. *Molecular Ecology*, **14**, 67–73.

Slatkin M, Excoffier L (1996) Testing for linkage disequilibrium in genotypic data using the Expectation-Maximization algorithm. *Heredity*, **76**, 377–383.

Smith P, Gaffney PM (2000) Toothfish stock structure revealed with DNA methods. *Water and Atmosphere*, **8**, 17–18.

Smith PJ, Gaffney PM (2005) Low genetic diversity in the Antarctic toothfish (*Dissostichus mawsoni*) observed with mitochondrial and intron DNA markers. *CCAMLR Science*, **12**, 43–51.

Smith P, McVeagh M (2000) Allozyme and microsatellite DNA markers of toothfish population structure in the Southern Ocean. *Journal of Fish Biology*, **57**, 72–83.

Sturmbauer C, Baric S, Salzburger W, Rüber L, Verheyen E (2001) Lake level fluctuations synchronize genetic divergences of cichlid fishes in African lakes. *Molecular Biology and Evolution*, **18**, 144–154.

Susana E, Papetti C, Barbisan F *et al*. (2007) Isolation and characterization of eight microsatellite loci in the icefish *Chaenocephalus aceratus* (Perciformes, Notothenioidei, Channichthyidae). *Molecular Ecology Notes*, **7**, 791–793.

Swearer SE, Shima JS, Hellberg ME *et al*. (2002) Evidence of self-recruitment in demersal marine populations. *Bulletin of Marine Science*, **70**, 251–271.

Swofford DL (2003) *PAUP*. Phylogenetic Analysis Using Parsimony (*and Other Methods)*, ed. 4.04a. Sinauer Associates, Sunderland, Massachusetts.

Thatje S, Hillenbrand CD, Mackensen A, Larter R (2008) Life hung by a thread: endurance of Antarctic fauna in glacial periods. *Ecology*, **89**, 682–692.

Thomas CD, Bodsworth EJ, Wilson RJ *et al*. (2001) Ecological and evolutionary processes at expanding range margins. *Nature*, **411**, 577–581.

Tomczak M, Godfrey JS (2003) *Regional Oceanography: An Introduction*. Daya Publications House, Delhi, India.

van Houdt JKJ, Hellemans B, van de Putte A, Koubbi P, Volckaert FAM (2006) Isolation and multiplex analysis of six polymorphic microsatellites in the Antarctic notothenioid fish, *Trematomus newnesi*. *Molecular Ecology Notes*, **6**, 157–159.

Van Oosterhout C, Hutchinson WF, Wills DPM, Shipley P (2004) Micro-Checker: software for identifying and correcting genotyping errors in microsatellite data. *Molecular Ecology Notes*, **4**, 535–538.

Volckaert FAM, Hänfling B, Hellemans B, Carvalho GR (2002) Timing of the population dynamics of bullhead *Cottus gobio* (Teleostei: Cottidae) during the Pleistocene. *Journal of Evolutionary Biology*, **15**, 930–944.

Wakeley J (2000) The effects of subdivision on the genetic divergence of populations and species. *Evolution*, **54**, 1092–1101.

White MG (1998) Development, dispersal and recruitment — a paradox for survival among Antarctic fish. In: *Fishes of Antarctica. A Biological Overview* (eds di Prisco G, Pisano E, Clarke A), pp. 53–62. Springer-Verlag Publishers, Milan, Italy.

Whitehouse MJ, Priddle J, Symon C (1996) Seasonal and annual change in seawater temperature, salinity, nutrient and chlorophyll a distributions around South Georgia, South Atlantic. *Deep Sea Research Part I: Oceanographic Research Papers*, **43**, 425–443.

Williams RC, Smolenski AJ, White RWG (1994) Mitochondrial DNA variation of *Champsocephalus gunnari* Lönnberg (Pisces: Channichthyidae) stocks on the Kerguelen Plateau, southern Indian Ocean. *Antarctic Science*, **6**, 347–352.

Won YJ, Hey J (2005) Divergence population genetics of chimpanzees. *Molecular Biology and Evolution*, **22**, 297–307.

Won YJ, Sivasundar A, Wang Y, Hey J (2005) On the origin of Lake Malawi cichlid species: a population genetic analysis of divergence. *Proceedings of the National Academy of Sciences, USA*, **102**, 6581–6586.

Wright S (1978) *Evolution and the Genetics of Populations*, Vol. 4. University of Chicago Press, Chicago, Illinois.

Zane L, Bargelloni L, Bortolotto E *et al*. (2006) Demographic history and population structure of the Antarctic silverfish *Pleuragramma antarcticum*. *Molecular Ecology*, **15**, 4499–4511.

Zane L, Ostellari L, Maccatrozzo L *et al*. (1998) Molecular evidence for genetic subdivision of Antarctic krill (*Euphausia superba* Dana) populations. *Proceedings of the Royal Society B: Biological Sciences*, **265**, 2387–2387.

Michael Matschiner is a doctoral student in the group of Walter Salzburger and interested in the molecular processes underlying adaptive radiation. Reinhold Hanel is head of the German Federal Research Institute of Fisheries Ecology (VTI/FOE) in Hamburg. He is a fish biologist interested in causes and pathways of adaptation and speciation in the sea. Walter Salzburger is Assistant Professor at the Zoological Institute of the University of Basel. The research of his team focuses on the understanding of the genetic basis of adaptation, evolutionary innovation and animal diversification. The laboratory's homepage at http://www.evolution.unibas.ch/salzburger provides further details on the group's (research) activities.

Supporting information

Additional supporting information may be found in the online version of this article:

Fig. S1 Statistical power tests for the mitochondrial control region data.

Fig. S2 Statistical power tests for the microsatellite data set.

Table S1 Locus name, repeat motif, forward (F) and reverse (R) primer sequences, fluorescent dye as well as PCR protocol details (Number of thermocycles and annealing temperatures, T_A) are reported for nine microsatellite loci

Table S2 Frequencies of haplotypes among populations

Table S3 Among group genetic differentiation, based on mtDNA and calculated by AMOVA

Table S4 Among group genetic differentiation, based on mtDNA and calculated by AMOVA

Table S5 Levels of genetic differentiation, as calculated by hierarchical AMOVA of mitochondrial D-loop sequences (10 000 permutations)

Table S6 p values of pairwise Φ_{STs} and F_{STs}, based on mtDNA (below diagonal) and microsatellites (above diagonal)

Table S7 Diversity indices for nine microsatellite loci

Table S8 Among group genetic differentiation, based on eight microsatellites and calculated by AMOVA

Table S9 Levels of genetic differentiation in eight microsatellite loci, calculated by means of hierarchical AMOVA (10 000 permutations)

Table S10 Estimated log probabilities of the microsatellite data, given the number of assumed genetic clusters, K, in the data set.

Please note: Wiley-Blackwell are not responsible for the content or functionality of any supporting materials supplied by the authors. Any queries (other than missing material) should be directed to the corresponding author for the article.